ELSEVIER
Spectrochimica Acta Part B xx (2007) xxx–xxx
SPECTROCHIMICA ACTA PART B
www.elsevier.com/locate/sab

μ-SXRF microprobe trace element studies on spherules of the Cretaceous/Tertiary boundary transitions of NE-Mexico and Haiti samples

Utz Kramar [a,*], Markus Harting [b], Karen Rickers [c,d], Doris Stüben [a]

[a] Universität Karlsruhe (TH), Institut für Mineralogie und Geochemie, Kaiserstraße 12, D-76128 Karlsruhe, Germany
[b] Utrecht University, Department of Earthsciences, Budapestlaan 4, 3508 TA Utrecht, The Netherlands
[c] Hamburger Synchrotronstrahlungslabor HASYLAB at Deutsches Elektronen-Synchrotron DESY, Notkestraße 85, 22607 Hamburg, Germany
[d] GeoForschungsZentrum Potsdam, Division 4.1, Telegrafenberg, 14473 Potsdam, Germany

Received 27 March 2006; accepted 24 June 2007

Abstract

Synchrotron radiation, collimated to a μm scale was used for the determination of trace elements in micro-tektites and spherule material for the first time. The experimental set-up of the SXRF microprobe at beamline L at HASYLAB at DESY offers a suitable method for performing non-destructive in situ multi-element analysis focusing on spatial trace element distributions and mineral phases of the melted ejecta material from the Cretaceous/Tertiary boundary. The spatial distribution of trace elements was determined in melt inclusions as well as in phase transitions in selected parts of chlorite–smectite spherules and tektite glass material by using a beam with a diameter of 15 μm collimated with a glass capillary for line- and area scans as well as for single point measurements for elements with Z between 19 and 92. The analyzed spherules show alteration features but also zonation and carbonate inclusions, originating from the Chicxulub impact event. These initial results demonstrate the potential of μ-SXRF analysis for the discrimination of alteration and primary signals of the spherules and re-construction of their genetic evolution. It could be shown that the spherules represent a complex mixture of different materials from the subsurface at the Chicxulub impact site.

Keywords: μ-SXRF; Multi-elemental analysis; Spherule; Cretaceous/Tertiary boundary; Mexico; Thin-section preparation

1. Introduction

In geo- and environmental sciences the knowledge of spatial trace element distributions in solid materials is crucial for example for the determination of the formation conditions of minerals, fixation and release of toxic elements to the environment and the determination of source materials for example from tektites. Because of this the so-called microprobes have become increasingly important in geo- and environmental sciences.

Several of these methods use charged particles for the excitation of X-rays like electron microprobe analysis (EPMA) and particle induced X-ray emission (PIXE). Both methods achieve μm sized spots with detection limits at the 100 ng/μg level for EPMA and at the 10 ng/μg level for PIXE (e.g. [1]). The high energy transfer of charged particles to a very small sample volume may complicate the analysis of volatile elements or can induce changes of valence states. Sensitivity is a nearly smooth function of the atomic number [2].

Secondary ion mass spectrometry (SIMS) and laser ablation inductively-coupled plasma mass spectrometry (LA-ICP/MS) are based on sputtering the sample followed by mass spectrometry. Using SIMS and LA-ICP/MS spot sizes of a few μm to some tens of μm and detection limits at the μg/g level are achieved. Sensitivities vary from element to element and quantification is difficult because of matrix effects in the ion production process (e.g. [3]).

SXRF microprobe techniques use photons for excitation. Spot sizes at the μm level and detection limits at the sub μg/g level are achieved.

In this study synchrotron radiation, collimated to the μm scale is applied for the first time to determine trace elements in micro-tektites and spherule materials.

In contrast to electron microprobe analyses the relative detection limits of μ-SXRF are more than 100 times lower, and comparable to those of LA-ICP/MS [4]. Contrary to LA-ICP/MS,

* Corresponding author.
E-mail address: utz.kramar@img.uni-karlsruhe.de (U. Kramar).

0584-8547/$ - see front matter © 2007 Published by Elsevier B.V.
doi:10.1016/j.sab.2007.06.012

where the analyte is evaporated, μ-SXRF is non-destructive and allows further investigations on the same sample material to be made (e.g. major element determinations by electron microprobe or determinations of additional trace elements by LA-ICP/MS.).

Like in all XRF methods sensitivities are a smooth function of the atomic number. The physics governing the interaction of photons with matter is well understood, therefore quantification is relatively straightforward (e.g. [5]).

Since the first investigations on geoscientific material (e.g. [6,7]) by synchrotron radiation induced X-ray fluorescence analysis (SXRF) it has been developed to a helpful tool in earth sciences for non-destructive, space resolved quantitative analysis of trace elements in the pg/μg range on a microscopic scale (e.g. [5,8,9]) of terrestrial [10–13]) as well as of extraterrestrial sample material [15,16]. Beamline L of the Hamburger Synchrotronstrahlungslabor at the Deutsches Elektronen-Synchrotron has been continuously used since 1994 for different applications of magmatic [16–23] and of sedimentary materials [20,24,25], as well as in experimental petrology [26–28]. In this study μ-SXRF was used for the determination of the spatial trace element distributions in tektite material from the Cretaceous/Tertiary boundary transition (K/T boundary) to re-construct their origin in relation to the Chicxulub impact event (late Mesozoic to early Cenozoic). The occurrence of tektite layers some 8–10m below the K/T boundary, which possibly represent the original layers, started a discussion that the Chicxulub impact may predate the K/T-boundary event by 300,000years [29,30].

2. Material, method and experimental set-up

2.1. Material and sample preparation

Spherule rich sediments were collected from the bedrock of the K/T-boundary transitions Bochil, Mesa-Juan Perez (detailed description in [31]) and Beloc (NE-Mexico and Haiti). Tektite material (Spherules) was collected from reworked Spherule layers near the K/T boundary as well as from the original tektite layer some 8–10m below the K/T boundary.

Samples were disaggregated, screened to the fractions >2 mm, 2 mm to 500 μm, 500 to 200 μm, 200 to 50 μm, and 50 to 20 μm (dry or wet using deionized water) and separated manually under the microscope. For disaggregation the Copper-(II)-sulfate treatment [32,33] was used. After disaggregation the samples were rinsed 3 times with deionized water to remove the surface contamination from the copper sulfate. During the preparation of the thin sections the spherules were cut and polished. Therefore any possible surface contamination was effectively removed. Since the synchrotron radiation with the set-up used penetrates the specimen at an angle of 45°, the radiation interacts with the matter of the sample along a cylinder of the beam diameter and a length depending on the radiation energy at lower energies or with a length of $d^*\sqrt{2}$ at high energies (above ~30keV). From this cylinder as well the characteristic X-rays as coherent and incoherent scattered X-rays reach the detector. The samples therefore have to be as thin as possible, in practice 80–110 μm to achieve the desired spatial resolution and lower limits of detection in the μg/g range.

As well as the short penetration depth of the beam in the sample, the advantages of very thin, self-supporting and doubly-polished thin sections are an easier positioning of grain boundaries in the synchrotron beam and a considerable reduction of background from scattered radiation (Rayleigh and Compton scattering of the sample matrix). Since in quantitative μ-SXRF the sample thickness has to be constant and known [34,35] the procedure for preparing self-supporting thin sections was modified to enable the preparation of slides with a constant thickness between 50 and 110 μm from loose packed spherule materials. To stabilize the fragile spherule material it was embedded in a resin (e.g. Araldite 2020 A/B®, Keorapox 439®, Epo-Tek®, Loctite UV®, UHU®, TESA®), which was stabilized with quartz powder in order to minimize the hardness contrast of the embedding resin and the embedded material. This enables polished surfaces on geological/paleontological materials of variable hardness to be prepared. The resin embedded spherules were then mounted on the carrier glass using an acetone-removable glue.

In the first step the sample was shaped and polished on one side and then removed for polishing of the other side. By using a modified resin there is no stability problem up to a thickness of 60 μm. In an experimental attempt a minimum thickness of less than 11 μm for an unsupported thin section could be achieved.

After glueing and stabilizing of the sample using Loctite UV®, the slides were polished by grinding the first layer in three steps to a flat area by using 600, 800 and 1200 grain size (graining). In a final step a Logitech PM2a spinner with WG2 polishing accessory and a 6 μm finish was used to generate a smooth and wave less surface which is necessary for quantitative determinations by μ-SXRF. For subsequent major element determination (up to atomic number 11) by electron microprobe analysis, the sample has subsequently to be finished using 3, 1 and 1/4 μm grain sizes. After fixing the rear side on a second sample carrier using UV-glue the first sample carrier is removed mechanically. Now the rear side of the thin section is polished as described, using the same grain sizes as mentioned above. Partial damage of the sample material and the embedding matrix is possible due to raw grains of the coarse grained polishing material. To avoid this effect it is necessary to work with the recommended, modified resin of adjusted hardness. The lapping of the second layer was stopped after optical checks of abraded sample material and changed to the Logitech PM2a polisher by using 6, 3, 1 up to 1/4 μm grain size for a minimum time of 25min each. The accurate processing of the surface is essential, because this surface will be the bottom layer after unfixing of the slide for the processing of the top layer. Cuts of spherule-rich rocks were also prepared as well as separated spherule material. After polishing and removing the sample from the carrier glass using acetone of p.a. quality (pro-analysis grade), the polished side was fixed on the carrier glass using UV-glue, the polishing procedure was repeated for the rear side. Depending on the material it is also possible to use other glues (e.g. UHU®, Tesa®) based on polyurethane composition, dissolvable by organic solvents. It is necessary, however, to prevent contamination of the sample by the preparation method. Every batch of glues, resins or tapes were tested for

Please cite this article as: U. Kramar et al., μ-SXRF microprobe trace element studies on spherules of the Cretaceous/Tertiary boundary transitions of NE-Mexico and Haiti samples, Spectrochim. Acta Part B (2007), doi:10.1016/j.sab.2007.06.012

t1.1 Table 1
Detection limits (D.L.) for the applied measurement conditions for the MPI-Ding-StHs6 reference material and for bulk EDXRF in typical geological t1.2 samples

t1.3 Element	Line	μ-SXRF D.L. in μg/g	EXDRF D.L. in μg/g
t1.4 Cu	K_α	4	5
t1.5 Zn	K_α	2.5	4
t1.6 Ga	K_α	2	3
t1.7 Rb	K_α	1.	1
t1.8 Sr	K_α	0.8	1
t1.9 Y	K_α	3	3
t1.10 Zr	K_α	1.3	2
t1.11 Nb	K_α	1	1
t1.12 Ba	K_α	2.5	3
t1.13 La	K_α	2.5	5
t1.14 Ce	K_α	3	5
t1.15 Pb	L_α/L_β	3	5

t1.16 Calculated for measuring times of 1000s.

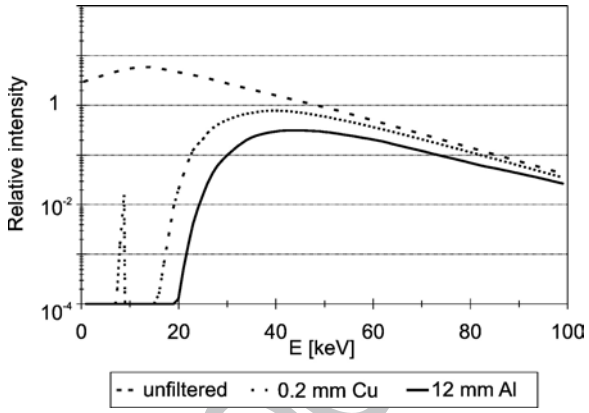

Fig. 2. Energy distribution of unfiltered and Cu- and Al-filtered synchrotron radiation used for the excitation of K-lines from elements with Z up to 82 (relative photon intensities vs. *E* (keV)).

their trace element contents before use. Trace element contents of all glues and resins used were tested by energy-dispersive X-ray fluorescence (EDXRF). Trace element contents of Araldite 2020 A/B®, Keorapox 439®, Epo-Tek®, UHU®, TESA® and Loctite UV® were found to be below the detection limits of EDXRF (Table 1) and therefore blanks of the used embedding materials did not disturb the measurements.

2.2. Experimental set-up

For trace element analysis μ-SXRF was used. X-ray fluorescence is an analytical tool in which an incident X-ray beam causes characteristic fluorescence in the sample. Basically, the intensities of the fluorescence lines are proportional to the concentrations of the excited elements. Consequently, the X-ray fluorescence technique may be applied for quantitative analysis if the absorption of the primary beam and the fluorescence radiation in the matrix is taken into account. Compared to conventional XRF methods using an X-ray tube as the photon source, the use of synchrotron radiation as a photon source has the advantage that it is characterized by much higher intensities and a low divergence of the primary beam. These spectrum characteristics enable trace element analysis at a high spatial resolution facilitating trace element distribution analysis within minerals. Further advantages are that the method is non-destructive and allows repeatability measurements.

The experiments were performed at HASYLAB Beamline L (Fig. 1) using the white beam for micro-X-ray fluorescence [36]. The synchrotron radiation at DORIS III originates from positrons with 4.5GeV at a bending magnet with a radius of 12.12m. The critical energy is 16.6keV. Above the critical energy, the intensity of the primary beam decreases rapidly, but up to 90keV the intensity is still sufficient for the detection of elements via K-shell excitation with Z up to 82 at trace element levels (Fig. 2). Due to the high energy part of the excitation spectra, high Z-elements can be analyzed by their K-lines instead of by their L-lines, which has the advantage that no or reduced peak overlaps occur for example in the determination of rare earth elements (REE). The incident beam was collimated down to a diameter of 15 μm by using a cross-slit system and a subsequent collimating glass capillary. The low energy part of the excitation spectrum was reduced by the use of different

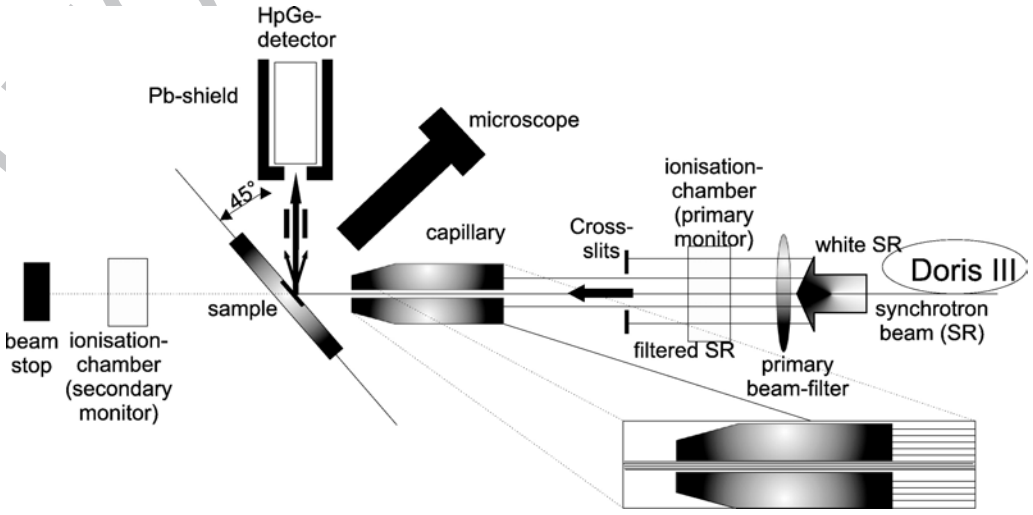

Fig. 1. Schematic diagram of the micro X-ray fluorescence set-up for white beam mode at HASYLAB at DESY (Hamburg).

Please cite this article as: U. Kramar et al., μ-SXRF microprobe trace element studies on spherules of the Cretaceous/Tertiary boundary transitions of NE-Mexico and Haiti samples, Spectrochim. Acta Part B (2007), doi:10.1016/j.sab.2007.06.012

absorbers (Cu 0.2 mm and Al 12 mm) in order to optimize the excitation spectra with respect to peak/background ratios of the characteristic X-ray lines of the analyte and to reduce the detector dead time. The energy spectrum of the white radiation and the Cu- and Al-filtered synchrotron radiation is shown in Fig. 2. The fluorescence spectra of the samples were measured using an energy-dispersive Hp-Ge detector with an active area of 30 mm^2, 5 mm thickness, and an energy resolution of FWHM 220eV at 5.9keV. The detector was arranged at an angle of 90° to the primary beam. Spectra accumulation times were 300s for single point measurements and between 150 and 300s per pixel for area- and line-scan measurements.

2.3. Data evaluation

For a given intensity and energy distribution of the primary beam the detected intensities of the X-ray lines of the different elements mainly depend on the concentration of the respective elements, path length of the primary and secondary radiation within the sample, density and matrix composition of the substrate, the energy of the respective X-ray line and the detector efficiency at the given energy.

Due to the symmetrical angles between the sample surface and the incoming primary beam and the surface and the outgoing fluorescence radiation, respectively, the total measured intensity of the X-ray line can be described as follows (e.g. [37]):

$$I_{(E)} = \int_0^x k_i I_0 c_i \rho \ \ \mathrm{e}^{\{-(\mu_0+\mu_i)\rho x\}} dx \qquad (1)$$

with k_i=proportionality constant for element i for fixed excitation conditions, ρ=density of the substrate, μ_0=mass attenuation coefficient of the primary radiation, μ_i=mass attenuation coefficient of the respective X-ray line of element i, x=effective path length of primary and secondary radiation in the sample and c_i=concentration of element i in the sample.

By integration of Eq. (1) the concentration c_i becomes

$$c_i = I_{(E)}(\mu_0 + \mu_i)/\{k_i I_0 \ (1 - \exp\{-(\mu_0 + \mu_i)\rho x\})\}. \qquad (2)$$

In effectively infinite thick samples this equation simplifies to

$$c_i = I_\infty(\mu_0 + \mu_i)/(k_i I_0) \qquad (3)$$

and for thin layers, where absorption within the layer can be neglected

$$c_i = I_{(E)}/(k_i I_0 \rho x). \qquad (4)$$

Depending on the thickness, density, matrix composition of the material and the radiation energy of the respective X-ray line, either the more general form (2) or one of the simplified forms (3) or (4) can be applied to calculate the concentration of the respective element in thin sections as used in μ-SXRF as long as the material can be considered homogeneous along the path of the incoming and outgoing radiation with respect to elements of concentrations >1%. This can be assumed for the central part if the diameter of the mineral grain is >200 μm. In the range of the grain boundaries (starting ~100μ in front of the grain boundary) the emitted X-rays are absorbed by both matrices. In cases where the matrix of the two phases is strongly different in their Fe or Ca contents this may cause systematic deviations in the range of the grain boundaries. These effects can be corrected by iterative methods like Monte Carlo simulation but for this a complete mathematical description of grain shape has to be developed and the knowledge of all major element concentrations and of the density of both mineral phases is necessary.

The fraction of the emitted intensity which is absorbed on its path to the surface even in a specimen of 100 μm thickness determines if the sample is to be considered as infinitely thick with concentrations calculated using Eq. (3), or as a thin layer,

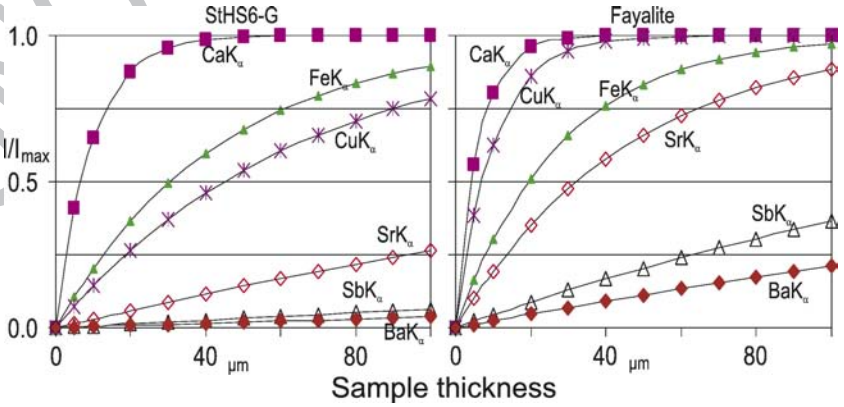

Fig. 3. Fraction of saturation intensity calculated for Ca, Fe, Cu, Rb, Zr and Ba-K_α lines using mass absorption coefficients from [38] in MPI-DING reference glass StHs6/80-G and in fayalite as a function of thickness of thin section. Note: for K-lines of Ca (3.7keV) saturation thickness is practically obtained within slides >50 μm while thin layer conditions can be assumed for K-lines of Ba (~32keV) and absorption within the thin section can be neglected. For K-lines with energies between ~5 and 25keV, saturation intensity is not obtained within thin sections of 100 μm thickness therefore thickness and matrix dependent absorption has to be taken into account.

Please cite this article as: U. Kramar et al., μ-SXRF microprobe trace element studies on spherules of the Cretaceous/Tertiary boundary transitions of NE-Mexico and Haiti samples, Spectrochim. Acta Part B (2007), doi:10.1016/j.sab.2007.06.012

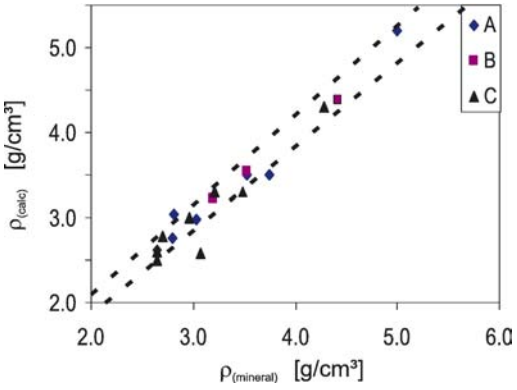

Fig. 4. Comparison of mineral densities [53] and densities calculated from Fe and Ca contents using Eq. (5) for crustal silicates (A), Eq. (7) for mantle and high pressure minerals (B) and Eq. (6) for alteration products (C). The dashed lines mark deviations of 5rel% between calculated and real densities. Minerals used for the density calculation: (A) albite, anorthite, wollastonite, hornblende, ferrohastingsite, sphene, magnetite; (B) fayalite, hedenbergite, forsterite; (C) Fe-chlorite, biotite (Fe-rich and Fe-poor), glauconite, phlogopite, chrysotile, antigorite, goethite.

where concentrations are calculated using Eq. (4). In geological material samples X-rays up to 6.5keV, emitted at the rear side of the sample are absorbed up to more than 90%. Therefore a sample of 100 μm thickness is practically infinitely thick for K-lines of elements with atomic numbers up to 26 (Fe K_α). X-rays with energies above 26keV are absorbed by less than 12% in a layer of 100 μm thickness in a typical geological sample provided the Fe_2O_3 does not exceed 20%.

Cases in which a thin layer in the narrower sense does not exist can nevertheless be calculated using the thin layer function as long as the absorption lies in the lower half of the linear part of the absorption function. This is the case up to an absorption of ~20%, as for Ba K_α in fayalite. Calculation as a thin layer will result in a relative underestimation of ~10%.

Consequently the sample fulfills the requirements of a thin layer for K-lines of elements with atomic numbers above 51 (Sb K_α). The concentrations of elements with X-ray energies between 6.6 and 26keV have to be calculated by the more complex Eq. (2) considering sample thickness, mass absorption and density of the specimen.

Fig. 3 gives the fraction of the saturation intensity as a function of thickness for a homogeneous layer of MPI-DING reference glass StHs6/80-G [4] and forsterite calculated for Ca-, Fe, Cu-, Rb-, Zr- and Ba-K_α lines.

According to Eqs. (2)–(4) the intensity of the analyte line depends on the density and mass attenuation coefficient of the matrix. Consequently for the quantification of trace and major elements in varying matrices the major element composition has to be known or has to be determined for example by electron microprobe.

Silicate minerals consist of 40 to 50% oxygen, 16 to 53% Si and up to 25% Al or Mg. Therefore at least 56% of the matrix of silicate minerals remains constant. For energies above the Fe

Table 2
Mass absorption coefficients μ for K-lines of major and trace elements and varying composition of silicates and pure $CaCO_3$ calculated using absorption coefficients of [38–42]

	Al_2O_3	MgO	Na_2O	SiO_2	CaO	Fe_2O_3	Ca	Fe	Ni	Cu	Zn	Rb	Sr	Ba
	Sample composition [%]						μ [cm²/g]							
Rhyolitic	10%	10%	10%	70%	0%	0%	285	61.6	39.8	32.9	27.1	7.19	6.34	0.79
Albitic	20%	0%	12%	68%	0%	0%	287	61.9	40.0	33.1	27.2	7.21	6.35	0.79
Forster.	0%	60%		40%	0%	0%	269	58.0	37.5	30.9	25.4	6.78	6.02	0.75
Low Fe	20%	0%	5%	74%	0%	1%	291	62.9	43.0	35.6	29.3	7.84	6.91	0.85
Interm.	20%	0%	5%	70%		5%	289	62.6	52.2	43.1	35.5	9.80	8.61	1.04
Basaltic	20%	0%	5%	65%		10%	287	62.1	63.7	52.5	43.2	12.2	10.7	1.27
Anorthite	36%			44%	20%		231	50.0	32.3	26.7	21.9	5.82	5.14	0.64
StHs6	18%	2%	5%	64%	5%	4%	266	57.6	47.5	39.2	32.2	8.89	7.82	0.95
Forsterite		54%		41%		5%	271	58.5	49.2	40.5	33.3	9.25	8.17	0.99
Fayalite		3%		31%	1%	67%	268	58.9	196	160	132	40.4	35.2	3.93
Calcite	$CaCO_3$						110	132	85.8	70.4	58.1	17.8	15.3	1.65
	Sample composition [%]						μ (sample)/μ (Si_2O_5)							
Rhyolitic	10%	10%	10%	70%	0%	0%	1.03	1.03	1.03	1.02	1.02	1.03	1.03	1.02
Albitic	20%	0%	12%	68%	0%	0%	1.03	1.03	1.03	1.03	1.03	1.03	1.03	1.02
Forster.	0%	60%		40%	0%	0%	0.97	0.97	0.97	0.96	0.96	0.97	0.98	0.97
Low Fe	20%	0%	5%	74%	0%	1%	1.05	1.05	1.11	1.11	1.11	1.12	1.12	1.10
Interm.	20%	0%	5%	70%		5%	1.04	1.04	1.35	1.34	1.34	1.40	1.39	1.33
Basaltic	20%	0%	5%	65%		10%	1.03	1.04	1.64	1.63	1.63	1.75	1.74	1.63
Anorthite	36%			44%	20%		0.83	0.84	0.83	0.83	0.83	0.83	0.83	0.82
StHs6	18%	2%	5%	64%	5%	4%	0.96	0.96	1.23	1.22	1.22	1.27	1.27	1.21
Forsterite		54%		41%		5%	0.98	0.98	1.27	1.26	1.26	1.32	1.32	1.27
Fayalite		3%		31%	1%	67%	0.96	0.98	5.05	4.98	4.99	5.03	5.78	5.04
Calcite	$CaCO_3$						0.40	2.20	2.21	2.19	2.19	2.21	2.56	2.12

Generally absorption coefficients from the different references [38–42] and their ratios deviate less than 5rel% from the average. The upper part gives calculated mass attenuation coefficient for the indicated matrix composition. The lower part indicates the ratio of mass attenuation coefficients of the indicated matrix composition and Si_2O_5.

Please cite this article as: U. Kramar et al., μ-SXRF microprobe trace element studies on spherules of the Cretaceous/Tertiary boundary transitions of NE-Mexico and Haiti samples, Spectrochim. Acta Part B (2007), doi:10.1016/j.sab.2007.06.012

absorption edge mass absorption coefficients of Al and Mg are only 20 respectively 35% lower than the mass absorption coefficient of Si, whereas the absorption coefficients of K, Ca and Fe are higher by a factor 2.3 to 5.16. Therefore, in dense geological silicate samples variations of sample density and mass absorption coefficients for energies above 4keV are mainly controlled by the Fe, K and Ca content of the sample (Fig. 4). Thus, after optical inspection of the thin section by polarization microscopy to determine the fractions of silicates, carbonates or oxides, that are present, an approach in accordance with Eq. (2) can be applied. This approach was also used to correct matrix effect of the tektite material. Since the light elements cannot be determined by X-ray fluorescence under non-vacuum conditions, the mass absorption coefficients have to be estimated. For the silicate part of a sample the mass absorption coefficient of Si_2O_5 is a good estimate for varying concentrations of the oxides Na_2O, MgO, Al_2O_3 and SiO_2 in a silicate. Even the mass absorption coefficients of K, Ca, Ti, Mn and Fe-free minerals e.g. albite, forsterite or quartz deviate by less than 5% from the mass absorption coefficients of Si_2O_5, whereas even 1% of Fe_2O_3 increases the mass absorption coefficient by more than 10% (Table 2). Nevertheless K, Ca, Ti and Fe can be determined under non-vacuum conditions with sufficient accuracy for the calculation of the total mass absorption coefficients.

The trace element concentrations in spherule material were determined by a semi-empirical approach based on Eqs. (1), (2) and (3) using the mass absorption coefficients of Si_2O_5 for the light element matrix and of K, Ca, Ti and Fe for the heavy part of the matrix. If Eqs. (2) and (3) are used, the density of the sample has to be known. The density range of most Fe-poor silicate minerals is between 2.5 and 3.3. Beside the crystal structure the density depends mainly on the concentrations of the heavier elements in the mineral. The density of a silicate matches almost exactly the mixing line of the respective Fe-free silicate and Fe oxide or hydroxide as an end member (Fig. 4). Depending on the mineralogy the density can be estimated as

$$\rho_{\text{sample}} = \rho_{\text{quartz}} + c[\text{CaO}]^*\left(\rho_{\text{calcite}} - \rho_{\text{quartz}}\right)/44 + c[\text{Fe}_2\text{O}_3]^*\left(\rho_{\text{maghemite}} - \rho_{\text{quartz}}\right)/100 \quad (5)$$

for crustal silicates and

$$\rho_{\text{sample}} = \rho_{\text{quartz}} + c[\text{CaO}]^*\left(\rho_{\text{calcite}} - \rho_{\text{quartz}}\right)/44 + c[\text{Fe}_2\text{O}_3]^*\left(\rho_{\text{goethite}} - \rho_{\text{quartz}}\right) \quad (6)$$

for alteration products and

$$\rho_{\text{sample}} = \rho_{\text{forsterite}} + c[\text{CaO}]^*(\rho_{\text{calcite}} - \rho_{\text{forsterite}}) + c[\text{Fe}_2\text{O}_3]^*\left(\rho_{\text{maghemite}} - \rho_{\text{forsterite}}\right) \quad (7)$$

for high Mg bearing mantle minerals (olivine) and high pressure minerals.

Using these estimates the deviation from the density of the natural minerals is less than 5% in most cases (Fig. 4).

Based on the intensities of Fe and Ca, variations of mass attenuation coefficients and density were estimated for the respective location of the sample. The resulting attenuation coefficients and fractions of saturation thickness for the respective X-ray lines were used for the correction of matrix effects and the amount of the sample. The calibration curves were determined from 100 μm thin sections of MPI-DING reference glasses KL2-G, StHs6/80-G, ML3B-G, BM90/21-G, T1-G and ATHO-G using the values given in [4].

Detection limits (Table 1) were calculated based on MPI-Ding-StHs6 standard sample/reference material using the following equation:

$$\text{D.L.} = m \cdot 3 \cdot \text{sqrt}\left(1000^* R_{\text{Bckgr}}\right) \quad (8)$$

with

R_{Bckgr} = countrate of background$[\text{s}^{-1}]$.
m = slope of calibration line$[\mu\text{g/g s}^{-1}]$.

The precision of the analytical results depend mainly on the counting statistics, accuracy of the thickness and density estimate of the thin section and of the accuracy of the ratios of the mass absorption coefficients of the matrix elements and of the reference matrix Si_2O_5 for the different X-ray energies used for the calculation. The ratios for pure matrix elements calculated from different references [38–42] vary by 1 to 7rel%. Consequently for a contribution of an element up to 30% to the matrix the error resulting from mass absorption coefficient can be expected to be smaller than 2% relatively. Therefore beside the counting statistics the precision mainly depends on thickness variations and the deviation of the density estimate from the actual density. Both components are estimated to contribute to the total standard deviation by 10% of the value.

3. Results and discussion

In unsupported thin sections of 100 μm thickness of spherules and micro-tektites the elements Ca, Ti, Mn, Fe, Cu, Zn, As, Rb, Zr, Sr, Nb, Ba, La, Ce and Pb have been determined simultaneously using a filtered polychromatic beam and a collimating capillary with a spot size smaller than 15 × 21 μm for line and area scans. It must nevertheless be taken into account that the information about elements, emitting high X-ray energies, corresponds to the complete sample thickness (Fig. 3). For hard X-rays, this results in an analyzed cylindrical volume of 15 μm diameter and 140 μm length equivalent to $3*10^{-4}\text{mm}^3$ or ~1 μg.

Detection limits were determined from 100 μm thick thin sections of the MPI-DING reference samples StHs6/80G and ATHO-G [4], applying the same measuring conditions as for the micro-tektites and spherules. In repetitive point measurements of 300s each (3points) a precision of 1% to 5% was obtained for Cu, Zn, Ga, Rb, Sr, Ba, La and Ce. The precision calculated from the counting statistics is equivalent to the precision obtained from repetitive measurements. The StHs6/80G [4] has a similar chemical composition to the examined micro-tektites from Beloc. The detection limits achieved with the micro-focus are comparable to, or better than, those obtained for bulk EDXRF (Table 1). As examples the spectra of reference sample ATHO-G [4] and of a glass spherule (micro-tektite) from Beloc

Please cite this article as: U. Kramar et al., μ-SXRF microprobe trace element studies on spherules of the Cretaceous/Tertiary boundary transitions of NE-Mexico and Haiti samples, Spectrochim. Acta Part B (2007), doi:10.1016/j.sab.2007.06.012

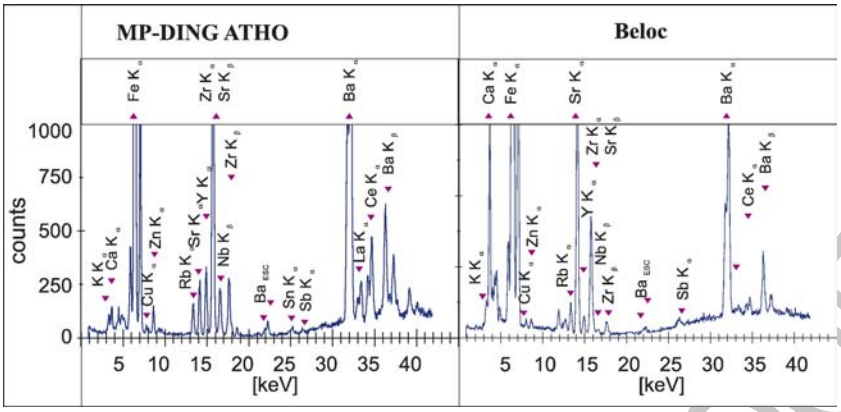

Fig. 5. X-ray fluorescence spectra of MPI-DING reference sample ATHO-G [4] and tektite glasses from Beloc/Haiti (white beam, 300s measuring time).

Haiti are given in Fig. 5. Compared to electron microprobe analysis the detection limits are 2–3 orders of magnitude lower, and even elements of high atomic numbers, for example rare earth elements, can be determined by their K-lines, where matrix effects are less important and spectral interferences are rare or easy to correct. PIXE reaches similar detection limits and spatial resolution as μ-SRXF, but the information remains restricted to the surface. LA-ICP/MS and SIMS reach similar detection limits, but the spatial resolution is lower in LA-ICP/MS, both methods are destructive and calibration is often more difficult because of severe matrix effects.

In this first study a total of 10 spherules from K/T sections Mesa-Juan Perez and Bochil in Mexico and Beloc in Haiti were measured and the major and trace elements Ca, Ti, Mn, Fe, Cu, Zn, As, Rb, Zr, Sr, Nb, Ba, La, Ce and Pb could be determined. Due to the high excitation energy of the polychromatic beam (up to 90keV) even Ba, La and Ce could be determined by their K-lines.

At Beloc (Haiti) two types of glass spherules are observed: "black" glasses with andesitic to dacitic composition and "yellow" glasses more enriched in Ca. The glasses (glass shards) from the Beloc section (Haiti) were mounted on micro-slides from former EPMA investigations. Due to the high penetration depth of the primary X-ray beam elements with higher atomic numbers, which are contained in the carrier glasses would be excited as well. Because of the relatively high trace element contents of the carrier glasses (e.g. several hundred μg/g As) the glass shards had to be removed from the support, reground and re-polished before they could be used for μ-SXRF. This resulted in uneven and lower thickness than the normally used value of 100 μm. Due to the varying thickness of the specimen a linear correlation of the apparent concentrations was observed for all elements which can be calculated by Eq. (3) (e.g. Rb, Sr, Ba, La, Ce), but not for the apparent concentrations of elements with low X-ray energies (e.g. Ca, Fe). For these light elements an apparent deviation from the linear trends is observed in the raw data (Fig. 6). To correct the thickness and matrix effect according to Eq. (1), the effective thickness at each point was determined from the count rate ratio of the primary and the secondary monitor (Fig. 1). The resulting trace element concentrations show a rather homogeneous distribution in the "black glasses" averaging at 6.3% CaO, 5.5% Fe_2O_3, 57 μg/g Zn, 57 μg/g, 614 μg/g Sr, 125 μg/g Zr, 474 μg/g Ba, 21 μg/g La and 44 μg/g Ce. These data are in good agreement with INAA data [43,44] for average black glasses of Beloc (Table 3). The "yellow" glasses more enriched in Ca show similar trace element patterns in comparison to "black" glasses poor in Ca (Cu, Zn, Zr, Y, Ba and REE) but by dilution due to carbonatic and evaporitic sediments trace elements except Sr lie at a slightly lower concentration level. The lower Ca- and Sr concentrations compared to the INAA and EPMA data [45] indicate that the yellow glasses measured in this study had incorporated a smaller fraction of carbonatic and evaporitic material.

These results demonstrate that variations of the specific intensity of the elements which are caused by uneven thickness of the specimen or by matrix effects can be corrected using the semi-empirical correction procedure based on ratios of primary and secondary monitor count rates and the intensities of the heavier major elements (Ca, Ti, Fe) as described above for silicate materials.

At most other locations, where micro-tektites from the K/T boundary were found, the glassy material is mostly altered or missing and fresh glasses are extremely rare. However, in some

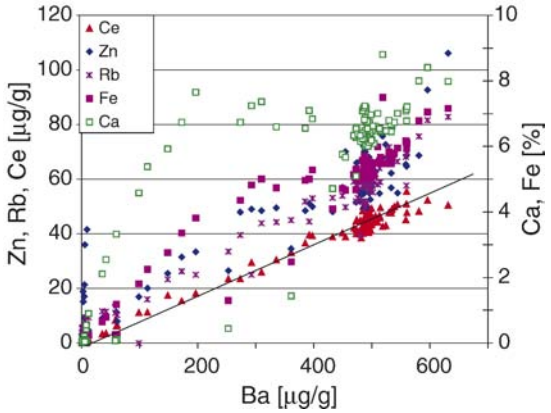

Fig. 6. Intensity correlation of Ba K-line (32.19keV) with K-lines (3.69 to 34.72keV) of elements with atomic numbers from 20 to 58 in a homogeneous micro-tektite (Beloc glass) of uneven thickness. For thin sections of 100 μm thickness thin layer conditions are fulfilled for Ba and Ce, whereas infinite thickness is fulfilled for Ca.

Please cite this article as: U. Kramar et al., μ-SXRF microprobe trace element studies on spherules of the Cretaceous/Tertiary boundary transitions of NE-Mexico and Haiti samples, Spectrochim. Acta Part B (2007), doi:10.1016/j.sab.2007.06.012

Table 3
Average concentrations of "black" and "yellow" Beloc glasses determined by μ-SXRF in comparison to literature data

Element		"Black" glass			"Yellow" glass		
		[45]	This work		[45]	This work	
CaO	[%]	6.52	6.3	±0.4	27	11.5	±0.7
Fe_2O_3	[%]	5.32	5.5	±0.5	4,91	6.3	±0.5
Cu	[μg/g]	n.d.	40	±7		27	±6
Zn	*[μg/g]*	*57*	*57*	±8	*50*	*53*	±8
Rb	*[μg/g]*	*45*			*17*	*40*	±5
Sr	*[μg/g]*	*550*	*624*	±65	*1620*	*901*	±90
Zr	*[μg/g]*	*110*	*125*	±15	*95*	*120*	±13
Ba	*[μg/g]*	*450*	*474*	±50	*550*	*380*	±40
La	*[μg/g]*	*20*	*21*	±4	*18*	*20*	±4
Ce	*[μg/g]*	*43*	*44*	±7	*37*	*38*	±7

of the investigated sections, almost fresh and unaltered glasses could be observed.

At these locations varieties of proximal ejecta for example smectite spherules with carbonate inclusions or Fe rich materials often with structures of melt Schlieren are observed. These materials often show signs of secondary alteration and it is difficult to decide whether the original patterns are mostly preserved or whether the fingerprints of the source materials have been destroyed completely. At Mesa-Juan Perez, for example, smectite spherules and extreme Fe- and Ca-rich spherules are observed. Some of the smectite spherules display carbonate inclusions and bubbles. One of these spherules, containing a carbonate rich inclusion with Schlieren structures and bubbles, was scanned in 20 μm steps along a 800 μm transect across the smectite material and inclusion (Fig. 7). Within the smectite two parts with characteristic trace element patterns were observed (Fig. 7): part A with higher concentrations of Zr (~100 μg/g), Ba (~200 μg/g), and Ce (10–20 μg/g) and low Rb (~5 μg/g) concentrations compared with part D showing higher concentrations of Rb (5 to 20 μg/g) and a depletion of Zr (~20 μg/g), Ba (~100 μg/g) and Ce (<5 μg/g). The distinct differences between parts A and D and the relatively constant concentrations levels within each of the two parts may indicate different source materials within the impact crater: a more detrital rich (A: higher Zr content) and more clay rich (D: higher Rb content).

During the alteration of glass or Zr-bearing minerals like amphibole, biotite etc., Zr will be released [46] but not included into the lattice of the newly formed alteration minerals. Due to its immobile behavior in low temperature fluids [46], Zr will not be transported over longer distances but tend to form its own trace minerals at phase boundaries. In line and area scan across the spherules, this will show up as Zr-"hot spots" at phase boundaries. Such "hot spots" (~400 μg/g Zr) were observed at the carbonate–smectite interface (F). At this phase boundary the highest Ba contents (~500 μg/g) were observed as well. Compared with the surrounding smectite, the carbonate inclusion (parts B and C) is relatively enriched in rare earth elements (up to 35 μg/g Y and Ce respectively), Ba (~400 μg/g) and Sr (500 to 1500 μg/g). This spherule obviously represents sediment material from the outer parts of the impact crater which was either molten at relatively low temperatures and not homogenized because of high viscosity or, analogous to carbonatite formation, carbonate and silicate phases separated from a silicatic–carbonatic melt due to liquid immiscibility during cooling down. The slow cooling rates which are necessary for those phase separations and the different trace element concentration levels of smectite parts A and D argue against the

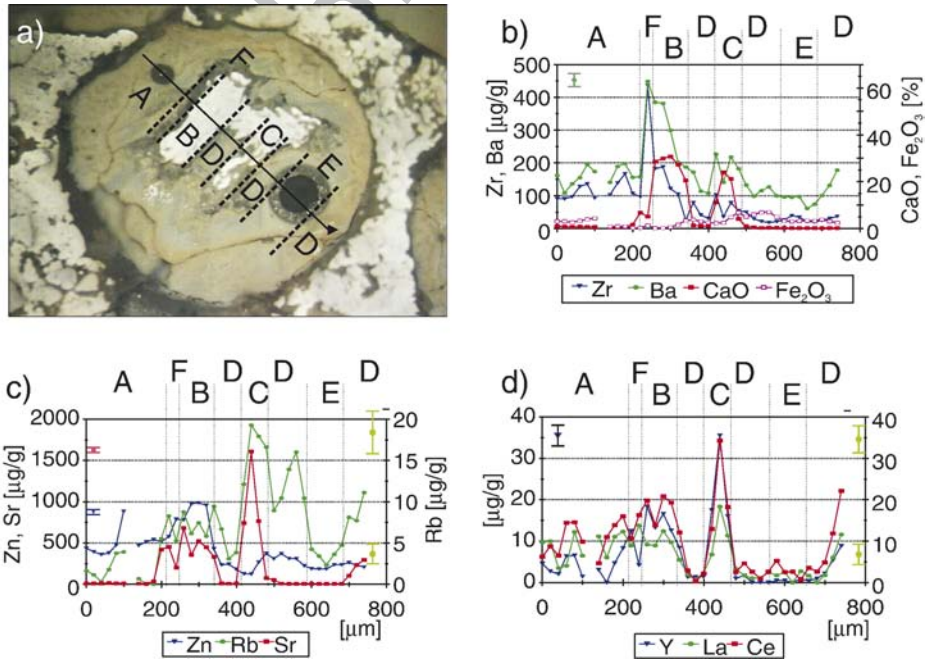

Fig. 7. Line scan of a spherule from the Mesa-Juan Perez section (NE-Mexico) with inclusion of $CaCO_3$ with Schlieren structures. a) micro-photograph of the spherule with indicated transect and zones of different concentrations and phases b–d) element profiles along the transect indicated in (a). Error bars are indicated for the standard deviation of the maximum concentrations. The standard deviation was calculated considering counting statistics, inaccuracies of the matrix correction procedure, inaccuracies in density calculation and thickness variations.

Please cite this article as: U. Kramar et al., μ-SXRF microprobe trace element studies on spherules of the Cretaceous/Tertiary boundary transitions of NE-Mexico and Haiti samples, Spectrochim. Acta Part B (2007), doi:10.1016/j.sab.2007.06.012

second type of formation. High Zn, Sr and REE contents of the carbonate inclusion indicate a non-diagenetic origin but the enrichment of Ba and Sr observed on the carbonate–smectite interfaces argues for re-crystallization.

Most spherules from Bochil section are strongly altered. An example of such an altered spherule is given in Fig. 8. Unlike the spherule from Mesa-Juan Perez, this spherule shows no sharp phase boundaries but gradually changing concentrations of Ca, Fe, Rb, Sr, and Ba, (Fig. 8). The highest concentrations of Ca (~7% CaO) are observed close to the outer boundary of the spherule.

The inner part of the spherule shows higher concentrations of Fe (up to 6% Fe_2O_3), Rb (~40 μg/g), Ba (200 to 400 μg/g). Beside a local enrichment of Sr together with Ca and a local Fe enrichment, both in to the outer part of the spherule, the spatial distributions of Rb, Sr and Ba resemble the distribution of Fe in general. The correlation of Fe, Rb, Sr, Ba, Zr and Nb may reflect the original trace element pattern of the smectite spherule while the absolute concentrations were changed due to alteration processes, mainly dissolution. The occurrence of high Zr concentrations together with the local Fe enrichment in the outer part of the spherule argues for trace element release during alteration of probably glassy material and re-precipitation of less mobile elements like Zr [41] in the outer parts. Elevated Ca concentrations in the outer part of the spherule compared to the inner part are an indication for impregnation of the spherule by secondary calcite. The gradually decreasing concentrations of most elements (Fe, Cu, Zn, Rb, Sr, Zr, Ba) from the innermost to the outermost parts of the spherule argues for intense alteration whereas the significant correlation of these elements is an indication that the trace element ratios are partly preserved while the absolute concentrations have changed. The inner part may show relicts of the original trace element contents but generally this spherule is overprinted by strong alteration, corrupting the primary signals.

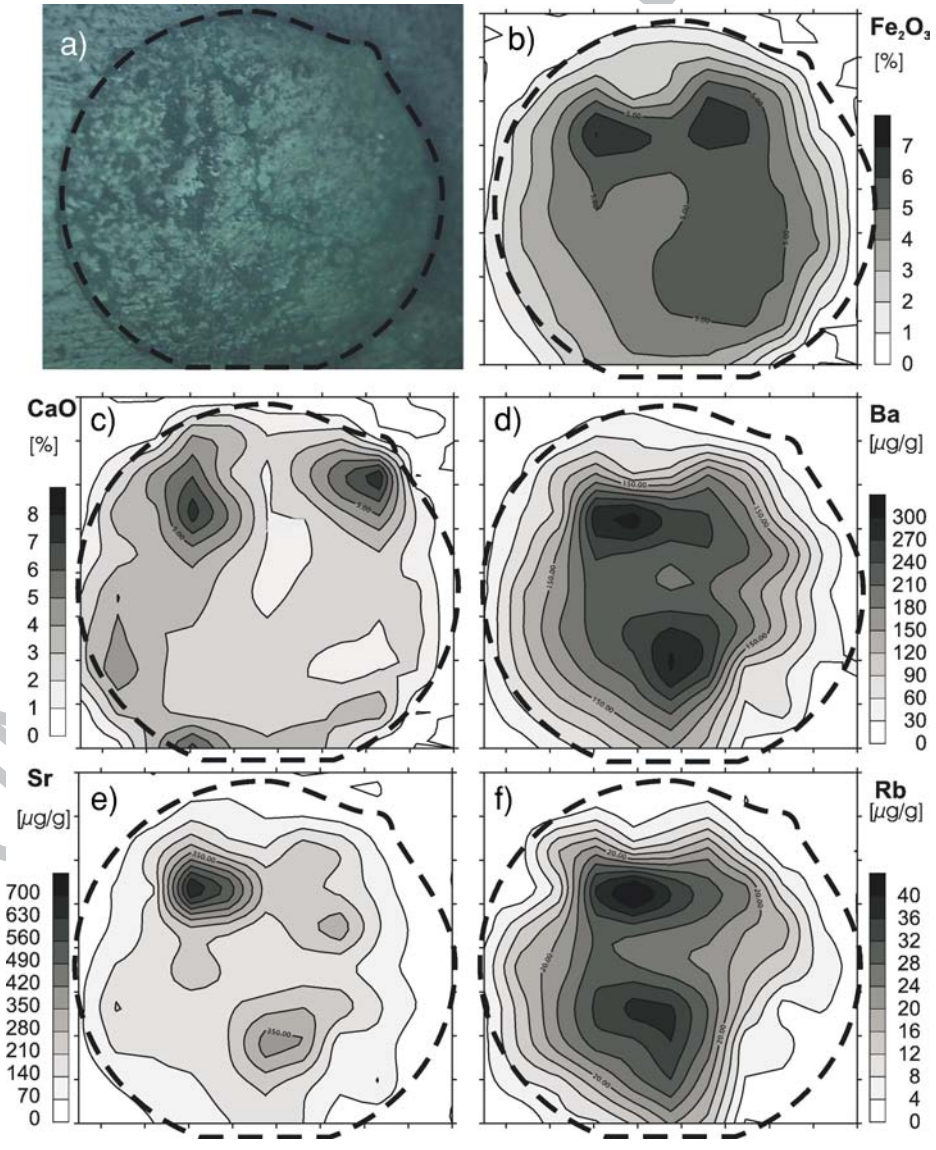

Fig. 8. Area scans of an altered tektite spherule from the Bochil (Mexico) section. a) Micro-photograph, b–f) distribution of CaO, Fe_2O_3, Sr, Ba and Rb within the spherule.

Please cite this article as: U. Kramar et al., μ-SXRF microprobe trace element studies on spherules of the Cretaceous/Tertiary boundary transitions of NE-Mexico and Haiti samples, Spectrochim. Acta Part B (2007), doi:10.1016/j.sab.2007.06.012

4. Summary and conclusions

μ-SXRF is the only non-destructive micro-analytical method which achieves the similar low detection limits as LA-ICP/MS. The high penetration depth of the X-rays used not only provides information from the surface of the sample but also from a depth up to several hundred μm. Because of this the method is less sensitive to surface contamination than the other micro-analytical methods. New focusing devices for X-rays (refractive X-ray lenses, polycapillaries) meanwhile allow smaller beam foci down to less than 100nm and the development of confocal optics enables the analysis of a defined sample volume at the spot position instead of a cylinder with varying length depending on the X-ray energy of the analyte element and true non-destructive 3-dimensional trace element analysis [47]. Nevertheless the use of refractive lenses and poly capillaries is restricted to monochromatic excitation beams. Theoretically CRLs can be used at energies up to some hundred keV but due to the low photon flux at high energies at bending magnet beamlines practical applications are limited to excitation energies of 30–50keV. In mineralogy and geology the rare earth elements (REE) are of high diagnostic importance. This is also the case for the re-construction of the micro-tektite parent materials.

- For the determination by their K-lines of Ba and REE's as diagnostic elements the excitation by a filtered white beam is more effective than excitation by the lower energies of the monochromatic beam.
- On the other hand, disadvantages of using the white beam in comparison to monochromatic excitation are poorer detection limits due to the higher background from scattered radiation.
- Quantification of X-ray fluorescence spectra is most often based on fundamental parameter procedures or on Monte Carlo simulation. For both methods the major elemental chemistry, sample geometry and density have to be known exactly, which often is not the case. The semi-empirical approach, which was used in this paper to correct matrix effects of mineralogical materials, is based on mass absorption coefficients of heavy major elements, average silicate mass absorption coefficients and monitor count rate ratios. In the case of elements that are emitting X-ray energies, which do not fulfill the conditions for infinite thickness in the specific thin section, the densities were corrected on the basis of the computed Fe and Ca concentrations. This reduces the effect of density variations on the results to less than 5%. The accuracy which can be achieved using this approach is of course not comparable to accuracies obtained by fundamental parameters in bulk analysis e.g. for quality control, but sufficiently exact for the determination of trace elements in inhomogeneous geological materials. For the homogeneous part of a mineral grain the uncertainty introduced by matrix and density variations is estimated to be better than 10rel% after correction. In trace element analysis cases the bigger in most uncertainty is the counting statistics. If all parameters are known the results obtained by using this semi-empirical approach have not the same accuracy but are comparable to those obtained by fundamental parameters or Monte Carlo simulations. However, and this is the advantage, this semi-empirical method does not require the knowledge of the complete major element chemistry and of the density. Care has to be taken in the region of grain boundaries, where the primary beam and the outgoing radiation may penetrate different matrix materials with drastic differences in the mass absorption coefficients e.g. Fe-oxides in contact with silicates. In such regions matrix effects are not considered adequately and the analytical data can only be considered as semi-quantitative, however the ratios of most trace element concentrations will not be affected. For the identification of possible source materials these elemental ratios are of much higher importance as the absolute values.

Spherules (micro-tektites) found in many K/T transitions are interpreted as ejecta material of the Chicxulub impact event near the K/T boundary some 65million years ago [43,48–52]. However, the origin of this tektite material and its chemical trace element composition is mainly unknown and at the moment not well studied. Space resolved trace element mapping by μ-SXRF enabled differentiation between altered and unaltered parts of the tektite spherules and the identification of the source rocks to be made by comparing trace element distribution patterns (fingerprints) of possible source rocks and spherules. The extreme differences in the chemical composition of spherules from different localities could not be simply explained by weathering of glass material from a homogeneous source.

- Glassy material for example of Beloc section (Haiti) is characterized by homogeneous trace element distribution patterns but shows characteristic differences between Ca-rich and Ca-poor glass. This is indicative of the mixing of different source materials from the impact crater. Major and trace element patterns indicate an origin from deeper crust material and minor amounts of evaporitic components mixed into the melt.
- Line and area scans from tektite material of Mesa-Juan Perez and Bochil section (Mexico) showed calcite inclusions, zonings or gradual changes of trace element contents. Based on the spatial trace element distribution some of these inclusions are indicative of primary material from the impact crater (example of Mesa-Juan Perez, Fig. 7). Trace and major elements indicate a sedimentary source of these spherules.
- Enrichments of Ca and other calcite related elements (Sr, Ba) in the outer parts of the micro-tektites represent impregnation by secondary calcite (e.g. Bochil, Fig. 8). These types of spherules are strongly overprinted by diagenesis. Nevertheless the original trace element ratios may be partly preserved.

Summarizing, the non-destructive determination of the spatial trace element distribution in micro-tektites on the μm scale by μ-SXRF enables differentiation between alteration rims, non-altered material and mixing of different source materials. This makes of μ-SXRF an extremely valuable tool to reconstruct the scenario of the K/T-boundary impact event. Q5

Please cite this article as: U. Kramar et al., μ-SXRF microprobe trace element studies on spherules of the Cretaceous/Tertiary boundary transitions of NE-Mexico and Haiti samples, Spectrochim. Acta Part B (2007), doi:10.1016/j.sab.2007.06.012

5. Uncited reference

[14]

Acknowledgements

This study was supported by the Deutsche Forschungsgemeinschaft (grants Stu 169/10-1-3). The sample material was provided by Gerta Keller and Wolfgang Stinnesbeck. We would also like to thank very much Stefan Höhne for the selection of spherule material of the Beloc section and the staff of the HASYLAB Synchrotron radiation facility for their assistance and the HASYLAB for providing beamtime at beamline L as well as Arndt Knöchel (Hamburg) for his encouragement to investigate our tektite material by μ-SXRF. We are grateful to Manfred Gerken, Kristian Nikoloski and Stefan Unrein for their help in thin section preparation and last but not the least our thanks go to Dirk Munsel and Ian Ray for improving our English. The comments of two anonymous reviewers have been also very helpful to improve the manuscript.

References

[1] A. Denker, J. Opitz-Coutureau, J.L. Campbell, J.A. Maxwell, T. Hopman, High-energy PIXE: quantitative analysis, Nucl. Instrum. Methods, Sect. B 219–220C (2004) 130.

[2] S.A.E. Johansson, J.L. Campbell, K.G. Malmqvist, Particle-Induced X-Ray Emission Spectrometry (PIXE), Wiley, New York, 2005.

[3] P.J. Potts, J.F.W. Bowles, S.J.B. Reed, M.R. Cave (Eds.), Microprobe Techniques in Earth Sciences, Chapman and Hall, London, 1995.

[4] K.P. Jochum, D.B. Dingwell, A. Rocholl, B. Stoll, A.W. Hofmann, et al., The preparation and preliminary characterisation of eight geological MPI-DING reference glasses for in-situ microanalysis, Geostand. Newsl. 24 (1) (2000) 87–133.

[5] S.R. Sutton, M.L. Rivers, P.J. Eng, M. Neville, Applications of synchrotron X-ray microprobe analysis in geochemistry and cosmochemistry, Eos, Trans. - Am. Geophys. Union 78 (1997) F789.

[6] A.V. Dubinin, I.I. Volkov, V.B. Baryshev, G.N. Kulipanov, X-ray fluorescence analysis by means of synchrotron radiation for rare-earth elements, yttrium, and barium in Pacific bottom sediments, Geochem. Int. 23 (1986) 61–68.

[7] J.D. Frantz, H.K. Mao, Y.G. Zhang, Y. Wu, A.C. Thompson, J.H. Underwood, R.D. Giauque, K.W. Jones, M.L. Rivers, Analysis of fluid inclusion by X-ray fluorescence using synchrotron radiation, Chem. Geol. 69 (1988) 235–244.

[8] J.V. Smith, M.L. Rivers, Synchrotron X-ray microanalysis, in: P.J. Potts, J.F.W. Bowles, S.J.B. Reed, M.R. Cave (Eds.), Microprobe Techniques in Earth Sciences, Chapman & Hall, London, 1995, pp. 163–233.

[9] N. Allison, A.A. Fincii, S.R. Sutton, M. Newville, Strontium heterogeneity and speciation in coral aragonite: implications for the strontium paleothermometer, Geochim. Cosmochim. Acta 65 (2001) 1669–2976.

[10] C. Dalpé, D.R. Baker, S.R. Sutton, Synchrotron X-ray-fluorescence and laser-ablation ICP-MS microprobes; useful instruments for analysis of experimental run-products, Can. Mineral. 33 (1995) 481–498.

[11] M.O. Figueiredo, T. Pereira da Silva, J.P. Veiga, P. Chevallier, Phosphatization of basaltic rocks from Sal Island, Cape Verde Archipelago: a microtopochemical approach using synchrotron radiation X-ray fluorescence, J. Phys. IV France 104 (2003) 399.

[12] M.J. Basto, Gold Assessment in Mics by XRF using synchrotron radiation, Chem. Geol. 124 (1995) 83–90.

[13] J. Rakovan, R. Reeder, Intercrystalline rare earth element distribution in apatite: surface structural influences on incorporation during growth, Geochim. Cosmochim. Acta 60 (1996) 4435–4445.

[14] A.H. Treiman, S.R. Sutton, Petrogenesis of the Zagami meteorite: inferences from synchrotron X-ray (SXRF) microprobe and electron microprobe analyses of pyroxenes, Geochem. Cosmochim. Acta 56 (1992) 4059–4074.

[15] G.J. Flynn, S.R. Sutton, L.P. Keller, Synchrotron X-ray fluorescence trace element measurements on interplanetary dust particles as a method to infer their sources and interrelationships, Lunar Planet. Sci. XXXIII (2002) 1648.

[16] T. Umsonst, R. Emmermann, J. Lauterjung, W. Bach, S. Garbe, M. Radtke, A. Knöchel, K. Janssens, L. Vincze, F. Adams, REE determination in mid ocean ridge basalts from the East Pacific Rise — results from synchrotron radiation induced X-ray fluorescence (SYXRF), HASYLAB Ann. Rep. (1994) 989–990.

[17] W. Bach, E. Hegner, J. Erzinger, M. Satir, Chemical and isotope variations along the superfast spreading East Pacific Rise from 6 to 30° S, Contrib. Mineral. Petrol. 116 (1994) 365–380.

[18] M.J. Streck, F. Lechtenberg, P. Sachs, H.U. Schmincke, Trace element concentrations obtained by synchrotron-XRF spot analysis for mineral partition coefficients of high-silica rhyolites, HASYLAB Ann. Rep. (1995) 945–946.

[19] A. Klügel, P.M. Sachs, F. Lechtenberg, H.U. Schmincke, Trace element zoning in mantel xenoliths: first results of synchrotron X-ray fluorescence analysis (SYXRF), HASYLAB Ann. Rep. (1995) 947–948.

[20] P.M. Sachs, T.H. Hansteen, Pleistocene underplating and metasomatism of the lower continental crust: a xenolith study, J. Petrol. 41 (2000) 331–356.

[21] V.R. Troll, U.-H. Schmincke, REE mineral perrierite/chevkinite in comenditic magmas from Gran Canaria, Spain: a SYXRF-probe study, J. Petrol. 43 (2002) 243–270.

[22] B. Bühn, A.H. Rankin, M. Radtke, M. Haller, A. Knöchel, Burbankite, a (Sr, REE, Na, Ca)-carbonate in fluid inclusions from carbonatite-derived fluids: identification and characterization using Laser Raman spectroscopy, SEM-EDX, and synchrotron micro-XRF analysis, Am. Mineral. 84 (1999) 1117.

[23] K. Rickers, R. Thomas, W. Heinrich, Trace-element analysis of individual synthetic and natural fluid inclusions with synchrotron radiation XRF using fundamental parameter quantification, Eur. J. Mineral. 16 (2004) 23–35.

[24] S. Hlawatsch, C.D. Garbe-Schönberg, F. Lechtenberg, A. Manceau, N. Tamura, D.A. Kulik, M. Kersten, Trace metal fluxes to ferromanganese nodules from the western Baltic Sea as a record for long-term environmental changes, Chem. Geol. 182 (2002) 697–709.

[25] J. Osán, S. Török, B. Alföldy, G. Falkenberg, Characterization of anthropogenic sediment particles after a transboundary water pollution of River Tisza using synchrotron radiation, Spectrochim. Acta Part B 59 (2004) 701–708.

[26] J. Koepke, H. Behrens, Trace element diffusion in andesitic melts: an application of synchrotron X-ray fluorescence analysis, Geochim. Cosmochim. Acta 65 (2001) 1481–1498.

[27] J. Koepke, G. Falkenberg, K. Rickers, O. Diedrich, Trace element diffusion and element partitioning between garnet and andesite melt using synchrotron X-ray fluorescence microanalysis (m-SRXRF), Eur. J. Mineral. 15 (2003) 883–892.

[28] C. Schmidt, K. Rickers, In-situ determination of mineral solubilities in fluids using a hydrothermal diamond-anvil cell and SR-XRF: solubility of AgCl in water, Am. Mineral. 88 (2003) 288–292.

[29] G. Keller, W. Stinnesbeck, T. Adatte, D. Stüben, Multiple impacts across the Cretaceous–Tertiary boundary, Earth-Sci. Rev. 62 (2003) 327–363.

[30] M. Harting, Zum Kreide/Tertiär-Übergang in NE-Mexiko: Geochemische Charakterisierung der Chicxulub-Impaktejekta. PhD Thesis Universität Karlsruhe, Fak. f. Bauingenieur-, Geo- und Umweltwissenschaften, 2004.

[31] D. Stüben, U. Kramar, M. Harting, W. Stinnesbeck, G. Keller, T. Adatte, High resolution geochemical record in Mexico during the Cretaceous–Tertiary transition, Geochim. Cosmochim. Acta 69 (2005) 2559–2579.

[32] G. Bourdon, Méthodé de dégagemet du microfossiles par acetolyse a chaude, Compte Rendu de la Societé Géologique de France, Paris, 1962, pp. 267–268.

[33] T. Nötzold, Die Präparation von Gyrogoniten und kalkigen Charophyten-Oogonien aus festen Kalkgesteinen, Monatsber. Deutsch. Akad. Wiss. Berlin 7 (1965) 216–221 (Berlin).

Please cite this article as: U. Kramar et al., μ-SXRF microprobe trace element studies on spherules of the Cretaceous/Tertiary boundary transitions of NE-Mexico and Haiti samples, Spectrochim. Acta Part B (2007), doi:10.1016/j.sab.2007.06.012

[34] D.R. Bessette, Analyse und Quantifizierung geologischer Proben mit der Synchrotron-Röntgenfluoreszenz, Diss. Universität Hamburg, 1999.
[35] R.S. Sutton, P.M. Bertsch, M. Newville, M. Rivers, A. Lanzirotti, P. Eng, Microfluorescence and microtomography analyses of heterogeneous earth and environmental material, in: P.A. Fenter, M.L. Rivers, N.C. Sturchio, S.R. Sutton (Eds.), Applications of Synchrotron Radiation in Low Temperature Geochemistry and Environmental Science, RiMG, vol. 49, 2002, pp. 429–483.
[36] F. Lechtenberg, S. Garbe, J. Bauch, D.B. Dingwell, F. Freitag, M. Haller, H.U. Hansteen, P. Ippach, A. Knöchel, M. Radtke, C. Romano, P.M. Sachs, H.U. Schmincke, H.J. Ullrich, The X-ray fluorescence measurement place at beamline L of HASYLAB, J. Trace Microprobe Tech. 14 (1996) 561–587.
[37] R. Jenkins, R.W. Gould, D. Gedcke, Quantitative X-ray Spectrometry, Marcel Dekker, New York, 1981.
[38] J. Leroux, T.P. Thinh, Revised Tables of X-ray Mass Attenuation Coefficients, CSC, Canada G1S 48N, 1977.
[39] C.T Chantler, K. Olsen, R.A. Dragoset, J. Chang, A.R. Kishore, S.A. Kotochigova, D.S. Zucker, X-Ray Form Factor, Attenuation and Scattering Tables (version 2.1). [Online] Available: http://physics.nist.gov/ffast [2007, January 12]. National Institute of Standards and Technology, Gaithersburg, MD. Originally published as Chantler, C.T., J. Phys. Chem. Ref. Data 29(4), 597–1048 (2000); and Chantler, C.T., J. Phys. Chem. Ref. Data 24, 71–643 (1995).
[40] R. Jenkins, J.L. de Vries, Practical X-ray Spectrometry, Macmillian Co Ltd., London-Basingstoke, 1970.
[41] K.L. Williams, Introduction to X-ray Spectrometry, Allen and Unwin, 1987.
[42] H. Hubbell, S.M. Seltzer, Tables of X-ray Mass Attenuation Coefficients and Mass Energy-Absorption Coefficients, NISTIR, vol. 5632, 1996.
[43] D. Stüben, U. Kramar, Z. Berner, J.D. Eckhardt, W. Stinnesbeck, G. Keller, T. Adatte, K. Heide, Two anomalies of platinum group elements above the Cretaceous–Tertiary boundary at Beloc, Haiti: geochemical context and consequences for the impact scenario, GSA Spec. Pap. 365 (2002) 163–188.
[44] H. Sigurdsson, R.M. Leckie, G.D. Acton, Shipboard scientific party: Caribbean volcanism, Cretaceous/Tertiary impact, and ocean climate history: synthesis of Leg 165, Proc. Oc. Drill. Prog. Initial Reports:, 1997, pp. 377–400.
[45] H. Sigurdsson, Ph. Bonte, L. Turpin, M. Chaussidon, N. Metrich, M. Steinberg, Ph. Pradel, S. D'Hondt, Geochemical constraints on source region of Cretaceous/Tertiary impact glasses, Nature 353 (1991) 839–842.
[46] B. Rasmussen, Zircon growth in very low grade metasedimentary rocks: evidence for zirconium mobility at ~ 250 °C, Contrib. Mineral. Petrol. 150 (2005) 146–155.
[47] C.G. Schroer, M. Kuhlmann, U.T. Hunger, T.F. Günzler, O. Kurapova, S. Feste, B. Lengeler, M. Drakopoulos, A. Somogyi, A.S. Simionovici, A. Snigirev, I. Snigireva, Nanofocusing parabolic refractive X-ray lenses, in Synchrotron Radiation Instrumentation, T. Warwick.
[48] P. Agrinier, A. Deutsch, U. Schärer, I. Martinez, Fast back-reactions of shock-released CO_2 from carbonates: an experimental approach, Geochim. Cosmochim. Acta 65 (2001) 2615–2632.
[49] A.P. Jones, P. Claeys, S. Heuschkel, Impact melting of carbonates from the Chicxulub, Lect. Notes Earth Sci. 91 (2000) 343–361.
[50] C. Koeberl, K.G. MacLeod (Eds.), Catastrophic Events and Mass Extinctions: Impacts and beyond, Geol. Soc. Am. Spec. Pap., vol. 356, 2002, pp. 1–746.
[51] B. Ivanov, A. Deutsch, The phase diagram of $CaCO_3$ in relation to shock compression and decomposition, Phys. Earth Planet. Inter. 129 (2002) 131–143.
[52] B. Kettrup, A. Deutsch, M. Ostermann, P. Agrinier, Chicxulub impactites: geochemical clues to the precursor rocks, Meteor. Planet. Sci. 35 (2000) 1229–1238.
[53] W.A. Deer, R.A. Howie, J. Zusman, An Introduction to the Rock Forming Minerals, 2nd ed., Longman, London, 1992.

Please cite this article as: U. Kramar et al., μ-SXRF microprobe trace element studies on spherules of the Cretaceous/Tertiary boundary transitions of NE-Mexico and Haiti samples, Spectrochim. Acta Part B (2007), doi:10.1016/j.sab.2007.06.012